Penerbit Akademia Baru

Journal of Advanced Research in Micro and Nano Engineering

Journal homepage:
https://www.akademiabaru.com/submit/index.php/armne/index
ISSN: 2756-8210

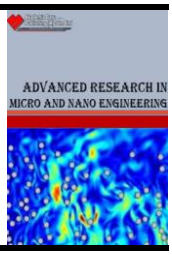

Polydimethylsiloxane-coated Fiber Bragg Grating as a Bend Sensor

Shazmil Azrai Sopian[1], Sumiaty Ambran[1,*], Nazirah Mohd Razali[1], Muhammad Quisar Lokman[1], Fauzan Ahmad[1], Nelidya Md Yusoff[2], Dwi Hanto[3]

[1] Malaysia-Japan International Institute of Technology (MJIIT), Universiti Teknologi Malaysia, Jalan Sultan Yahya Petra, 54100, Kuala Lumpur, Malaysia
[2] Razak Faculty of Technology and Informatics, Universiti Teknologi Malaysia, Jalan Sultan Yahya Petra, 54100 Kuala Lumpur, Malaysia
[3] Research Center for Photoncis, National Research and Innovation Agency, South Tangerang, Indonesia

ARTICLE INFO

Article history:
Received 23 December 2024
Received in revised form 17 January 2024
Accepted 19 February 2024
Available online 30 March 2024

Keywords:
Bend sensor; fiber Bragg grating; polydimethylsiloxane; sensitivity

ABSTRACT

The fiber Bragg grating sensor is often demonstrated as a bend sensor. However, the demonstrated sensor in previous studies was limited to low sensitivity, thus reducing the sensing performance. Hence, this work demonstrated the polydimethylsiloxane-coated fiber Bragg grating sensor for sensitivity enhancement. The proposed sensor with a diameter of 5 cm was bent by adjusting the translation stage from 0.1 cm to 0.9 cm distance in forward and backward direction. The results showed that the Bragg wavelength shifted towards the longer wavelength region when the distance decreased. The polydimethylsiloxane-coated fiber Bragg grating sensor shows a sensitivity of 1743000 A.U, 8 times higher than the uncoated fiber Bragg sensor with a sensitivity of 284000 A.U. The presence of the polydimethylsiloxane layer has successfully improved the sensor performance.

1. Introduction

The development of optical fiber sensors has been prompted by the advancement of optical fiber for communication technology [1]. The key benefits of fiber optic sensors are compact, passive, light, and immune to electromagnetic interference. Additionally, they have minimal power requirements, low attenuation, exhibit great sensitivity, wide bandwidth, and environmental toughness but the primary drawbacks are their high price and user unfamiliarity [2,3] .

Fiber Bragg grating (FBG) is a type of optical fiber sensor. Unlike normal optical fiber, FBG can reflect light at a certain wavelength mainly the so-called Bragg wavelength. It is very sensitive to strain. Hence, the sensor is often demonstrated as a bend sensor.

An overview of the FBG strain sensors is provided in this work. The study commenced with a measurement analysis, i.e., strain. Strain describes the displacement of particles in a substance to a reference length. It is a normalized measure of deformation. The strain is related to changes in the matter's size and shape as well as rigid body motions like translations and rotations [4]. The normal

* *Corresponding author.*
E-mail address: sumiaty.kl@utm.my

https://doi.org/10.37934/armne.17.1.105116

strain is known as tensile strain if the length of the body expands and compressive strain if it decreases [5].

In previous work, various optical technologies have been presented as bend sensors such as multi-core fiber (MCF) [6,7], long period fiber gratings (LPFGs) [7,8], fiber Bragg gratings (FBGs) [9, 10], photonic crystal fiber (PCF) [11,12], fiber tapers and fiber lateral-offset splicing [13-15]. The findings indicated that the measurement sensitivity is very low. Only a few sensors can identify three or more bending directions, which is insufficient for bending measurement. Most sensors are unable to distinguish directions or can only distinguish two opposed directions [16].

The preparation and performance testing of polydimethylsiloxane (PDMS) films are essential steps in the development of PDMS. Through the examination of the PDMS's fabrication process and characteristics, a film that can be loaded and unloaded repeatedly was created which is called a membrane [17]. It has the potential to be excellent biocompatibility and biologically relevant mechanical properties to serve as a coating for fibers. When integrated photonic circuits and circuits are being made [18-28] in an integrated system, PDMS is typically created into a unique waveguide [29,30]. Numerous studies have revealed that the PDMS-prepared integrated system has the qualities of low loss, high temperature stability, and sufficient mechanical stability. Then, there were rising concerns about the sensitive features of temperature and humidity. Numerous optical fiber waveguides composed entirely of PDMS were also developed at the same time [31,32]. Due to PDMS's excellent plasticity, optical waveguides can be easily constructed into a range of different forms, including knotted, twisted, and tapered fiber. The strain and temperature sensitivity of fiber sensors may be enhanced with PDMS [33].

This paper demonstrates the PDMS coated FBG as a bend sensor. The sensor operates at the near-infrared wavelength region ranging from 1510 nm to 1630 nm. The sensor performance was studied in both forward and backward flexibility. The sensor static characteristics, sensitivity and linearity were calculated and discussed.

2. Methodology

2.1 Polydimethylsiloxane Preparation

The PDMS was prepared by following the procedure in the previous literature [34,35]. Firstly, about 10 ml of epoxy (Slygard 184, Sigma Aldrich) and 1 ml of hardener (Curing Agent, Sigma Aldrich) were mixed into a disposable tube (refer to Figure 1). The mixture was stirred for 1 minute to remove the unwanted bubbles and to ensure the mixture was homogenous.

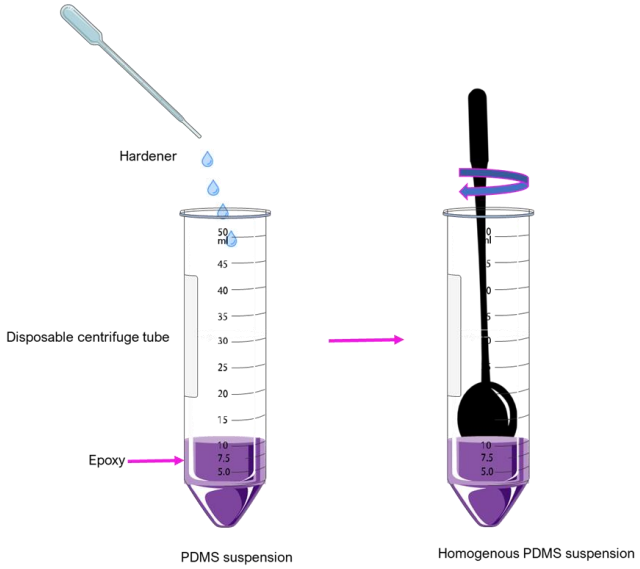

Fig. 1. Preparation of polydimehtylsiloxane (PDMS)

2.2 Coating Procedure Method

The FBG was first placed and fixed in the petri dish during the coating process. Next, the mixture was slowly poured into the petri dish and coated the whole FBG resulting in a 2 mm coat thickness. The alignment of the FBG is on the neutral axis of the PDMS membrane. Subsequently, the sample was left to dry at room temperature (27 °C) for 2 days. After that, the coated sample was taken out from the petri dish and trimmed to form a rectangular shape, as shown in Figure 2.

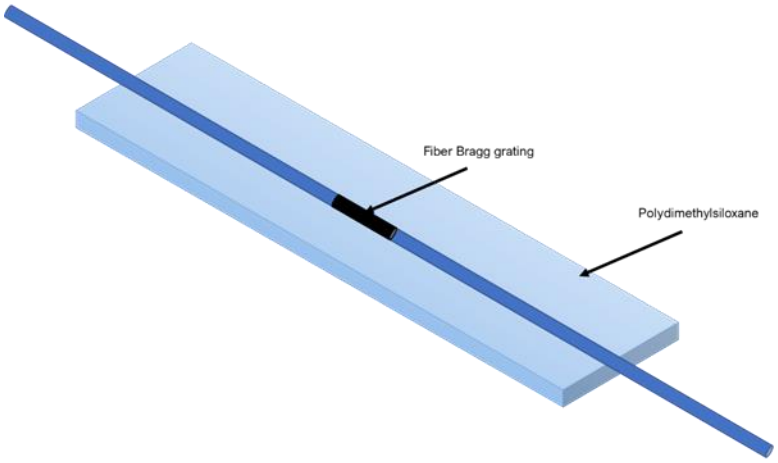

Fig. 2. PDMS coated FBG

2.3 Experimental Procedure

In the experiment, the PDMS-coated FBG sensor was fixed and placed on the translation stage as shown in Figure 3. The sensor was characterized by adjusting the distance ranging from 0.1 to 0.9 cm for the forward direction and 0.9 cm to 0.1 cm for the backward direction. The sensing system was excited using a broadband amplified spontaneous emission light source (ASE) (ASE FL7004, FiberLabs) ranging from 1530nm to 1610nm. The optical spectrum circulator was used to navigate the reflected

light from the sensor to the optical spectrum analyser (OSA) (AQ6370D, YOKOGAWA) to monitor the sensing spectrum changes.

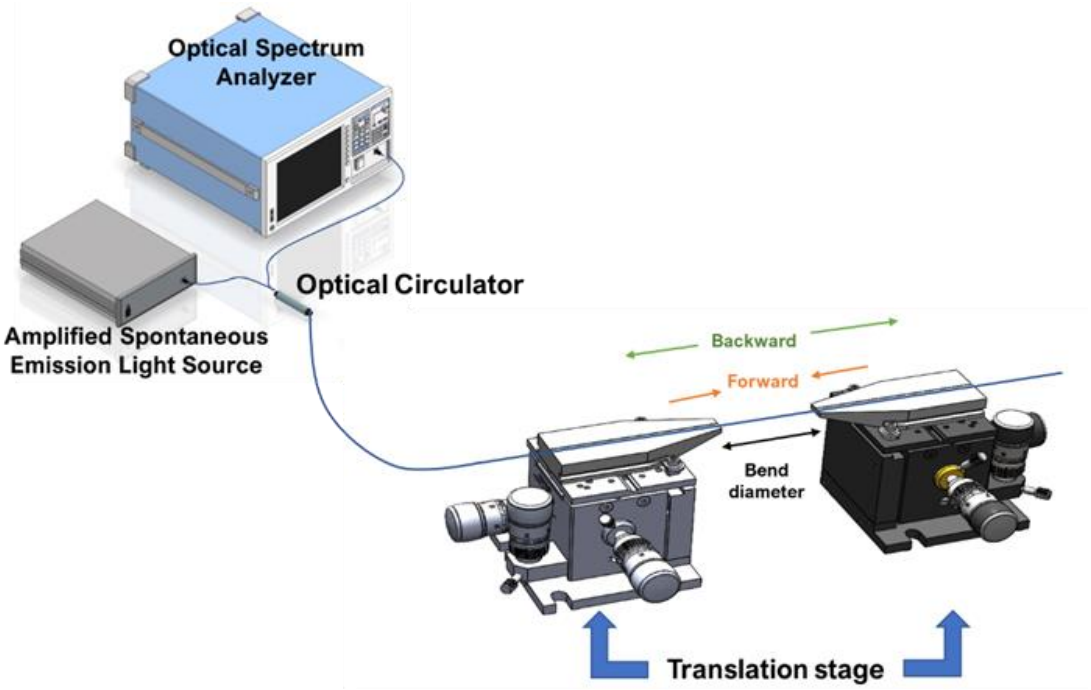

Fig. 3. Experimental setup

Figure 4 shows the procedure to adjust the fiber. Figure 4 shows the initial condition of the FBG, in the forward and backward directions.

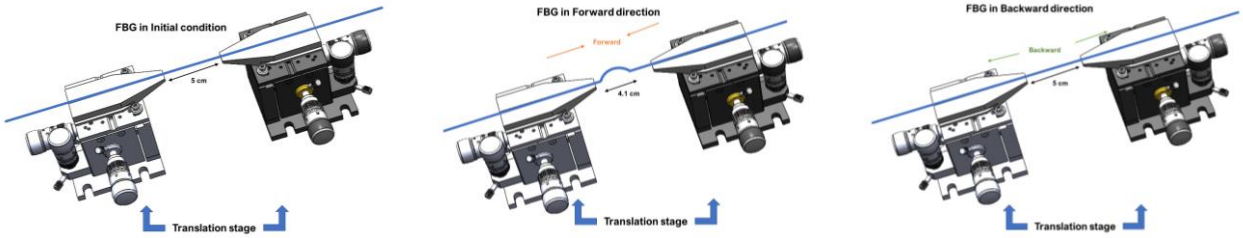

Fig. 4. shows the initial condition of the FBG, in the forward and backward directions

3. Results and Discussion

Figure 5 presents the sensing spectrum in the forward direction and the analysis of the shifting of Bragg wavelength from the distance of 0.1 cm to 0.9 cm for the first cycle of the experiment. As can be seen in Figure 5 (a), the spectrum fluctuates due to noise resulting in the data's instability. However, in Figure 5 (b), the spectrum became more stable as the FBG embedded in the PDMS. The Bragg wavelength shift was observed to be more prominent. In Figure 5 (a), the initial peak wavelength of uncoated FBG is 1549.8803 nm, which was increased to 1549.9024 nm, with a total increase of 0.0221 nm in the forward direction. The initial optical power loss is 13.15 dB was reduced to 13.1 dB, with a total power loss of 0.05 dB. In Figure 5 (b) the initial peak wavelength of PDMS-COATED FBG is 1550.1278 nm was increased to 1550.2716 nm, with a total increase of 0.1438 nm in the forward direction. The initial optical power loss is 14.42 dB was reduced to 14.39 dB, with a total power loss of 0.003 dB.

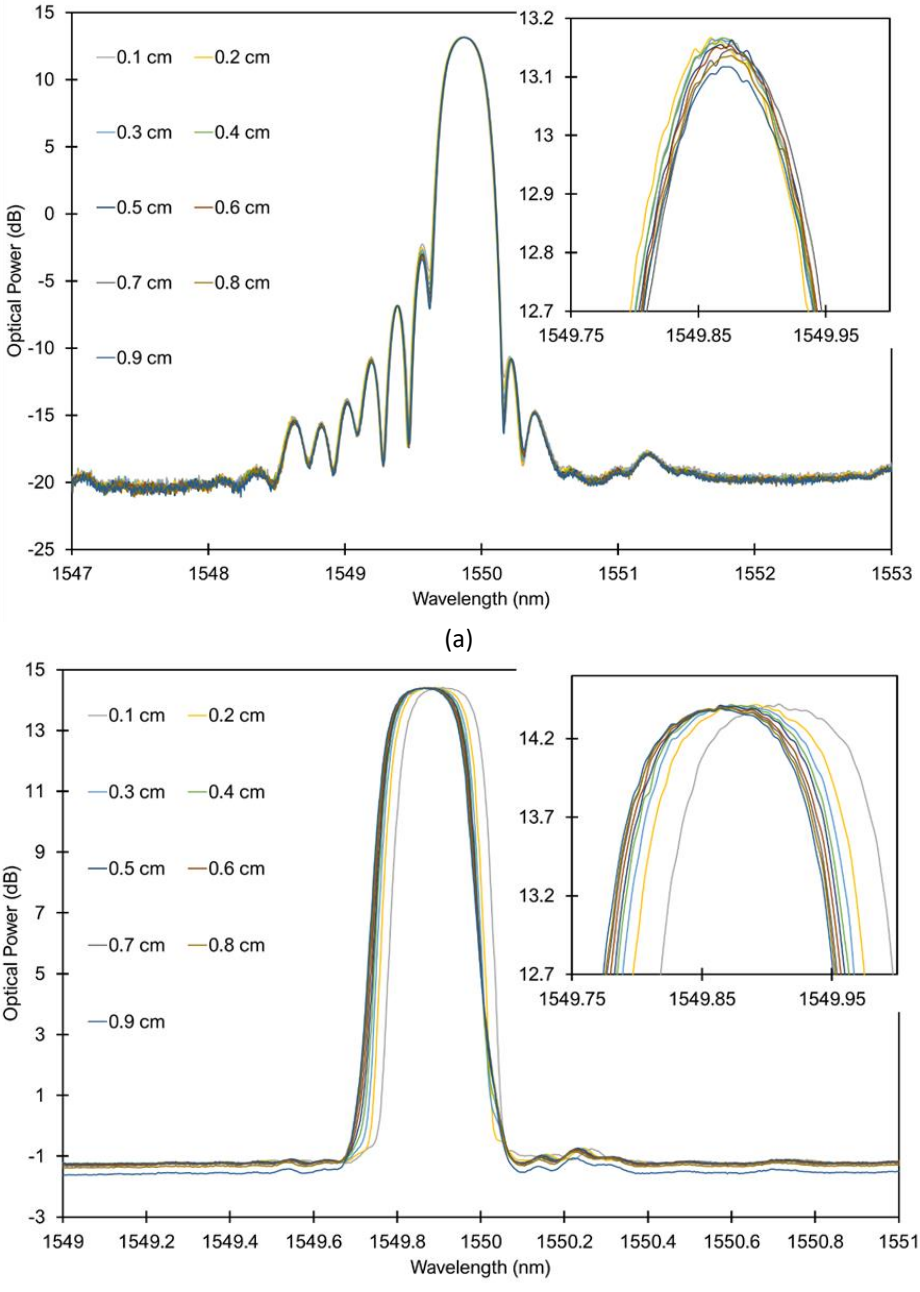

Fig. 5. The sensing spectrum of the (a) uncoated (b) coated in the forward direction

Figure 6 (a) depicts the Bragg wavelength shift, Δλ(nm), against the distance (cm) in the forward direction from 0.1 cm to 0.9 cm. In Figure 6 (a) uncoated FBG, as the distance of the diameter decreases from 0.1 cm to 0.9 cm, the uncoated Bragg wavelength shift increases from 0 Δλ(nm) to 0.0222 Δλ(nm) with the total change of 0.0222 Δλ(nm). A different trend can be seen in Figure 6 (a) PDMS-COATED FBG, as the distance of the diameter decreases from 0.1 cm to 0.9 cm, the coated Bragg wavelength shift increases from 0 Δλ(nm) to 0.1438 Δλ(nm) with the total change of 0.1438 Δλ(nm). In Figure 6 (a), the Bragg wavelength is linearly increasing with the decrease of the distance. The sensitivity achieved by uncoated FBG for the forward direction is 0.0284, Δλ(nm) with the linear regression value of 0. 9134. In comparison, the PDMS-COATED FBG sensitivity is 0.1743, Δλ(nm), with

a linear regression value of 0.9576. Table 2 summarizes the Bragg wavelength shifting for the forward direction.

Figure 6 (b) presents the optical power changes (dB) against the distance (cm) in the forward direction from 0.1 cm to 0.9 cm. For the uncoated FBG, as the diameter decreases, the optical power changes from -0.0733 dB to -1.97 dB with a total change of -1.8967. However, a different graph can be seen in Figure 6 (b) PDMS-COATED FBG. As the diameter decreases, the optical power changes increase drastically with the help of coated FBG, from -0.0933 dB to -0.2433 dB with a total change of -0.15 dB. In Figure 6 (b), uncoated FBG showed a subsequential change in the optical power dB, whereas the coated FBG showed only a slight change. The optical power changes of the PDMS-COATED FBG are higher than the uncoated FBG, which is -0.15 dB. Table 1 summarizes the optical power changes for the forward direction. In Figure 6 (b), the optical wavelength changes are linearly decreasing with the increase of the distance. The sensitivity achieved by uncoated FBG for the forward direction is -2.5372 dB/cm with a linear regression value of 0.9109. In contrast, the PDMS-COATED FBG sensitivity is -0.1617 dB/cm with a linear regression value of 0.0.837.

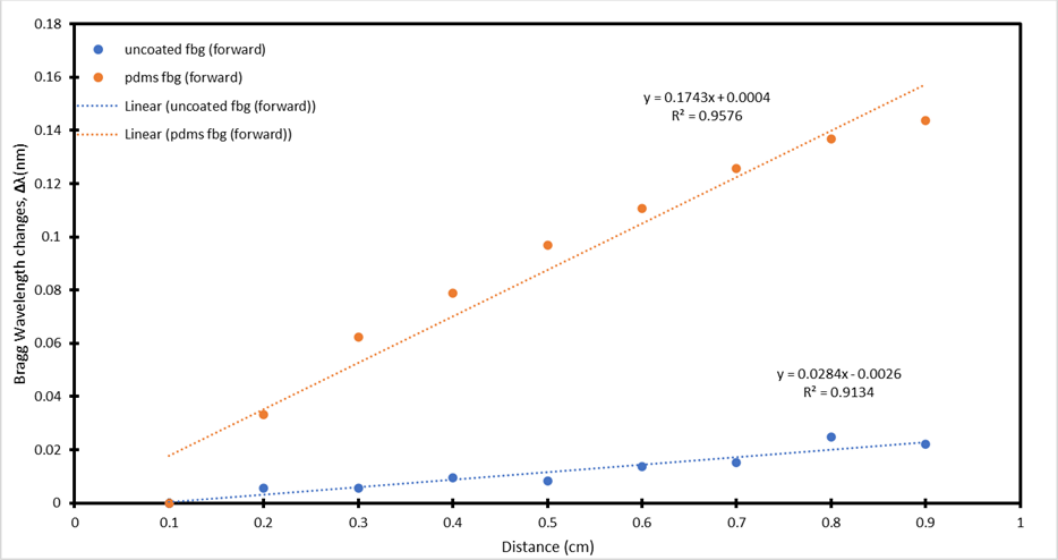

(a)

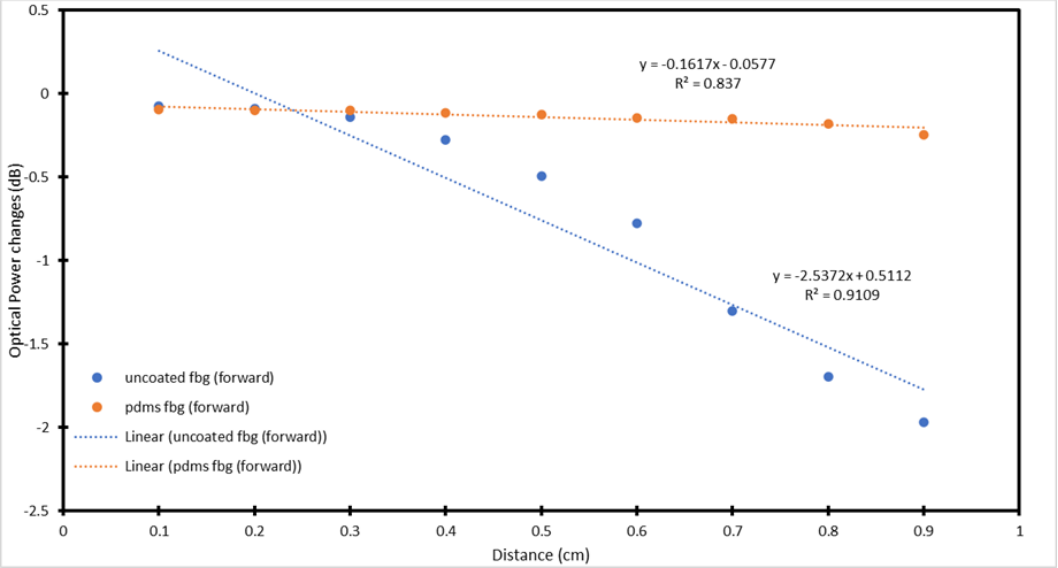

(b)

Fig. 6. The (a)Bragg wavelength shift (b) Optical power changes in the forward direction

3.1 Backward Direction

Figure 7 presents the sensing spectrum in the backward direction and the analysis of the shifting of Bragg wavelength from the distance of 0.9 cm to 0.1 cm for the first cycle of the experiment. As shown in Figure 7 (a), the spectrum fluctuates due to the noise resulting in the data's instability. However, in Figure 7 (b), the spectrum became more stable as the FBG embedded in the PDMS. The Bragg wavelength shift was observed to be more prominent. In Figure 7 (a), the initial peak wavelength of uncoated FBG is 1549.9024 nm was decreased to 1549.8801 nm, with a total decrease of 0.0223 nm in the backward direction. In comparison, the initial optical power is 13.11 dB, increasing to 13.16 dB, with a total power increase of 0.05 dB. In Figure 7 (b), the initial peak wavelength of PDMS-COATED FBG is 1550.2702 nm was decreased to 1550.1264 nm, with a total decrease of 0.1438 nm in the backward direction. In comparison, the initial optical power is 14.23 dB, which increased to 14.26 dB, with a total power increase of 0.003 dB.

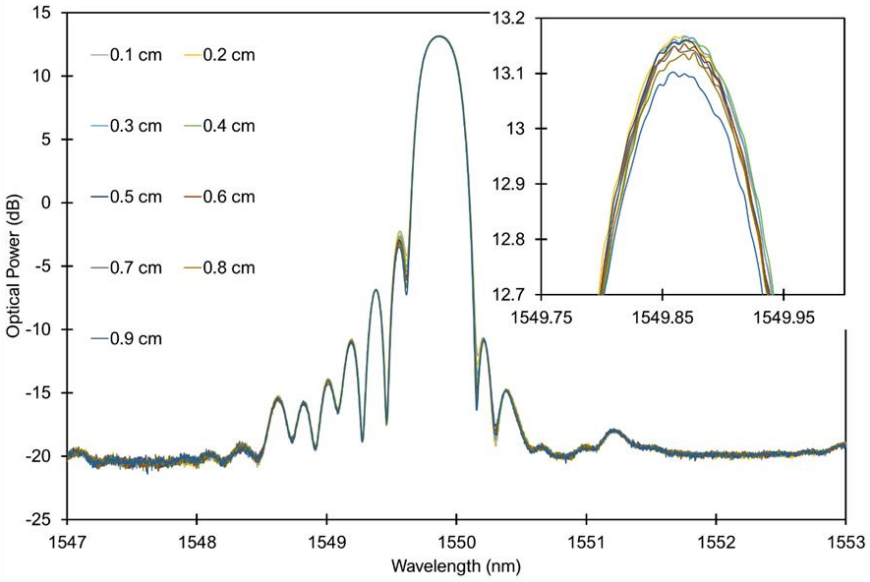

(a)

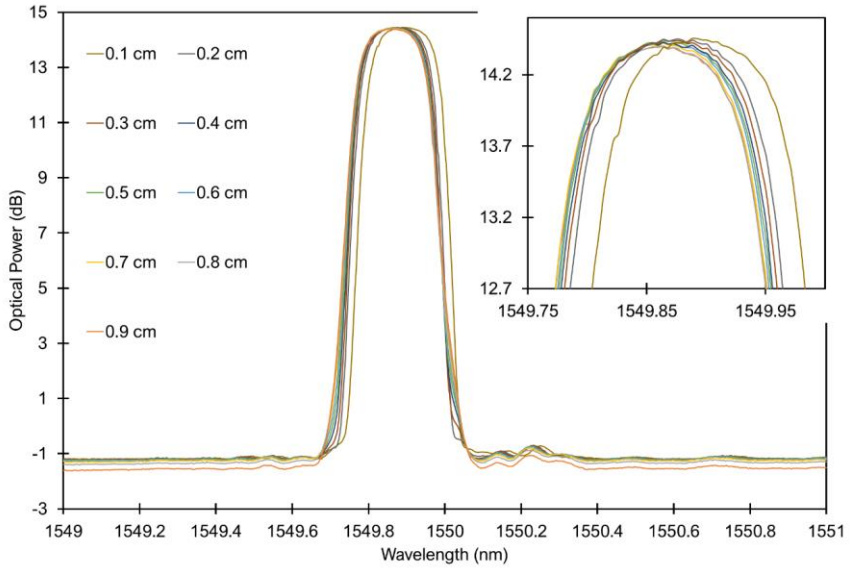

(b)

Fig. 7. The sensing spectrum of the (a) uncoated (b) coated in the backward direction

Figure 8 depicts the Bragg wavelength shift, Δλ(nm), against the distance (cm) in the backward direction from 0.9 cm to 0.1 cm. In Figure 8 (a) uncoated FBG, as the distance of the diameter increases from 0.9 cm to 0.1 cm, the uncoated Bragg wavelength shift increases from -0.0222 Δλ(nm) to 0 Δλ(nm) with the total change of 0.0222 Δλ(nm). A different trend can be seen in Figure 8 (a) PDMS-COATED FBG, as the distance of the diameter increases from 0.9 cm to 0.1 cm, the Bragg wavelength shift decreases from -0.1438 Δλ(nm) to 0 Δλ(nm) with the total change of 0.1438 Δλ(nm). In Figure 8 (a), the Bragg wavelength is linearly increasing with the increase of the distance. The sensitivity achieved by uncoated FBG for the forward direction is 0.7253, Δλ(nm) with a linear regression value of 0. 7253. In contrast, the PDMS-COATED FBG sensitivity is 0.0.1733 Δλ(nm) with a linear regression value of 0.9501. Table 2 summarizes the Bragg wavelength shifting for the backward direction.

Figure 8 (b) presents the optical power changes (dB) against the distance (cm) in the backward direction from 0.9 cm to 0.1 cm. For the uncoated FBG, as the diameter increases, the optical power changes from 0 dB to 1.83 dB, with a total change of 1.83. However, a different trend can be seen in Figure 8 (b) PDMS-COATED FBG. As the diameter increases, the optical power changes decrease from 0 dB to 0.1233 dB, with a total change of 0.1233 dB. In Figure 8 (b), uncoated FBG showed a subsequential change in the optical power dB, whereas the coated FBG showed only a slight change. The optical power changes of the PDMS-COATED FBG are lower than the uncoated FBG, which is 0.1233 dB. Table 2 summarizes the optical power changes for the backward direction. In Figure 8 (b), the optical wavelength changes are linearly decreasing with the increase of the distance. The sensitivity achieved by uncoated FBG for the forward direction is -2.3533 dB/cm with a linear regression value of 0.0.8648. In contrast, the PDMS-COATED FBG sensitivity is -0.1367 dB/cm with a linear regression value of 0.8199.

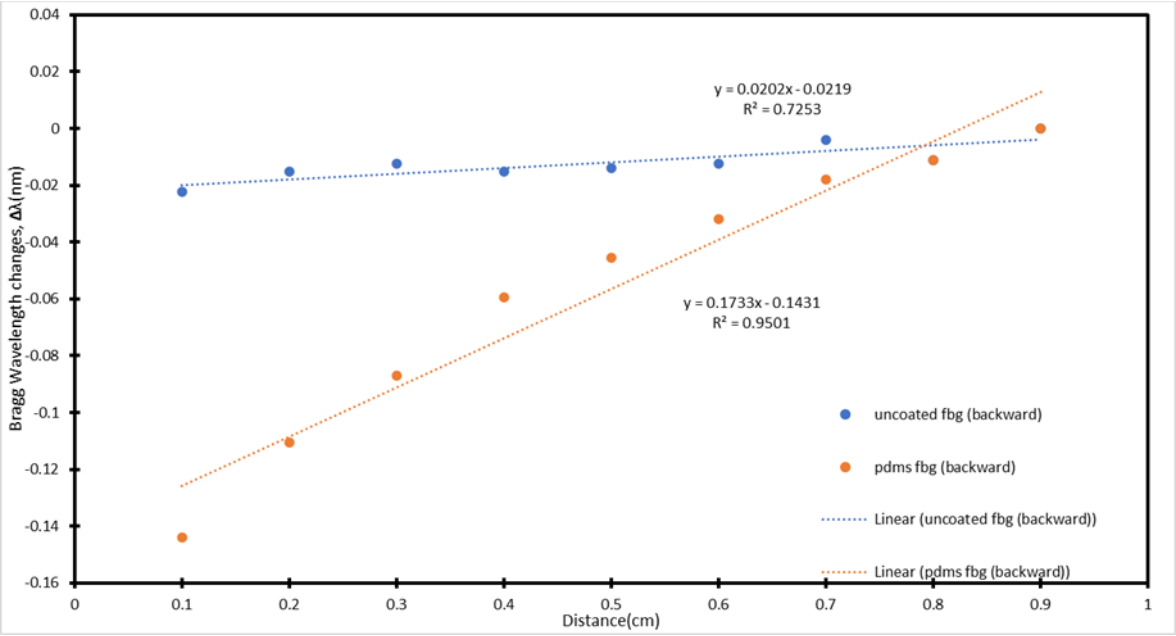

(a)

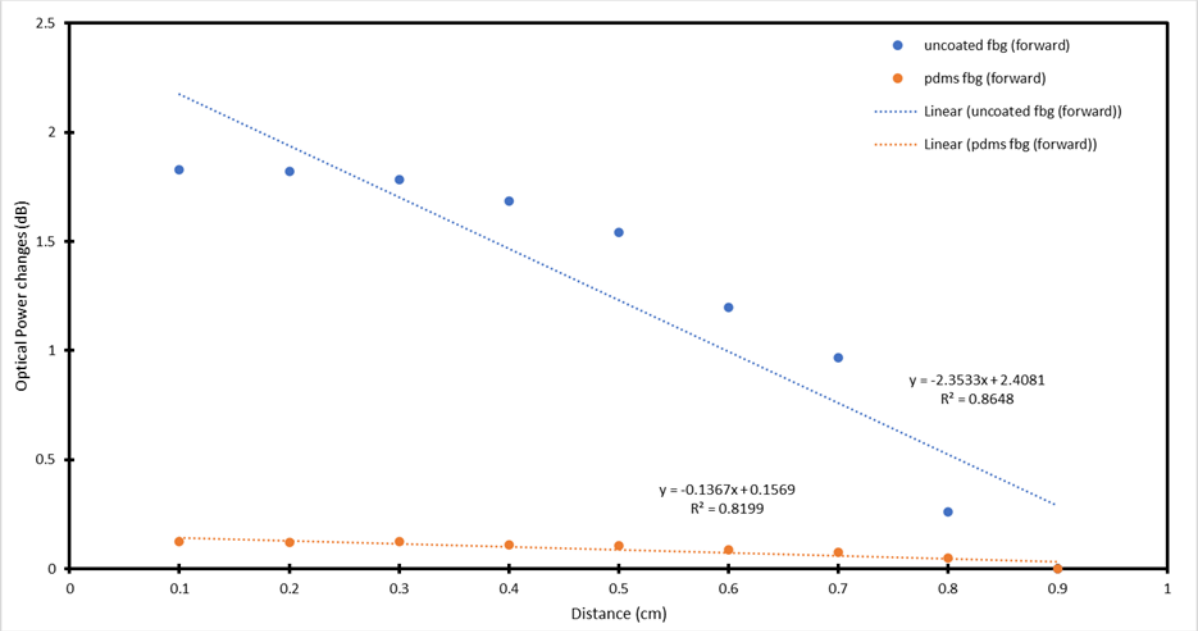

(b)

Fig. 8. The (a)Bragg wavelength shift (b) Optical power changes in the backward direction

Table 1 summarizes the FBG sensing performance based on optical power changes. The uncoated sensor shows a sensitivity of -2.5372 dB/cm and -2.3533 dB/cm in the forward and backward directions, respectively. Meanwhile, the PDMS coated FBG shows a sensitivity of -0.1617 dB/cm and -0.1367 dB/cm in the forward and backward directions, respectively. Even though the distance changes are similar for the uncoated FBG and PDMS coated FBG, slight changes can be observed from a short distance to longer distance, while the power is consistent and stable. Thus, this indicates that the Bragg wavelength shift can show significant changes and improve sensitivity. As for the optical power, the uncoated sensor shows the highest sensitivity compared to the PDMS coated FBG because the PDMS absorbed the power loss.

Table 1
FBG sensing performance based on optical power changes

Sensor	Forward sensitivity (dB/cm)	R^2	Backward sensitivity (dB/cm)	R^2	Measurement range (cm)
Uncoated	-2.5372	0.9109	-2.3533	0.8648	0.1-0.9
PDMS-COATED FBG	-0.1617	0.837	-0.1367	0.8199	

Table 2 summarizes the FBG sensing performance based on the Bragg wavelength shift. The uncoated sensor shows a sensitivity of 0.0284 nm/cm and 0.0202 nm/cm in the forward and backward directions, respectively. Meanwhile, the PDMS coated FBG shows a sensitivity of 0.1743 cm/nm and 0.1733 cm/nm in the forward and backward directions, respectively. The Bragg wavelength shift for the PDMS coated FBG sensor showed 8 times sensitivity higher than uncoated FBG.

Table 2
FBG sensing performance based on Bragg wavelength shift

Sensor	Forward sensitivity (nm/cm)	R^2	Backward sensitivity (nm/cm)	R^2	Measurement range (cm)
Uncoated	0.0284	0.9134	0.0202	0.7253	0.1-0.9
PDMS-COATED FBG	0.1743	0.9576	0.1733	0.9501	

The presence of PDMS has successfully improved the sensing performance. The PDMS coated FBG sensor shows a small sensitivity for the optical power changes because the PDMS layer absorbs the light loss penetrating the cladding region during bending. Thus, the PDMS coated sensor can rely on the Bragg wavelength shift without the optical intensity compensation. Next, the mechanical properties of the PDMS, such as strong and flexible, have improved the sensor feasibility by providing high sensitivity sensing performance. Furthermore, this can be seen in Table 2, in which the PDMS coated FBG sensor offers a larger wavelength shift compared to the uncoated sensor.

4. Conclusions

In conclusion, the PDMS-COATED FBG sensor can be an attractive candidate for bending purposes. Furthermore, the PDMS-COATED FBG sensor has been successfully introduced for strain measurement. The FBG sensor is embedded in PDMS elastomer, making the structure more stable and easier to handle. It also increases sensitivity and reduces bend loss. The strain can be measured by the application of bending, thus affecting the Bragg wavelength. The sensitivity of uncoated fiber Bragg grating in the forward direction exhibits a sensitivity of 0.0284 nm/cm and linearity of 0.9134. In contrast, the polydimethylsiloxane fiber Bragg grating indicates a sensitivity of 0.1743 nm/cm and linearity of 0.9576. The finding indicated that Fiber Bragg grating with polydimethylsiloxane could improve the sensitivity by 8 times.

Acknowledgement
This research was financially supported by University Grant Vot. No 20J91.

References
[1] Venghaus, Herbert, and Norbert Grote, eds. *Fibre optic communication: key devices*. Vol. 161. Springer, 2017. https://doi.org/10.1007/978-3-319-42367-8
[2] Yin, Shizhuo, Paul B. Ruffin, and T. S. Francis, eds. *Fiber optic sensors*. CRC press, 2017. https://doi.org/10.1201/9781420053661
[3] Jeunhomme, Luc B. *Single-Mode Fiber Optics: Prinicples and Applications*. Routledge, 2019. https://doi.org/10.1201/9780203739662
[4] Voyiadjis, George, and Mohammadreza Yaghoobi. *Size effects in plasticity: from macro to nano*. Academic Press, 2019.
[5] Kang, Guozheng, and Qianhua Kan. *Cyclic plasticity of engineering materials: experiments and models*. John Wiley & Sons, 2017. https://doi.org/10.1002/9781119180838
[6] Holmes, Christopher, Sumiaty Ambran, Peter A. Cooper, Andrew S. Webb, James C. Gates, Corin BE Gawith, Jayanta K. Sahu, and Peter GR Smith. "Bend monitoring and refractive index sensing using flat fibre and multicore Bragg gratings." *Measurement Science and Technology* 31, no. 8 (2020): 085203. https://doi.org/10.1088/1361-6501/ab8710
[7] Khan, Fouzia, Alper Denasi, David Barrera, Javier Madrigal, Salvador Sales, and Sarthak Misra. "Multi-core optical fibers with Bragg gratings as shape sensor for flexible medical instruments." *IEEE sensors journal* 19, no. 14 (2019): 5878-5884. https://doi.org/10.1109/JSEN.2019.2905010
[8] Zhang, Yun-Shan, Wei-Gang Zhang, Lei Chen, Yan-Xin Zhang, Song Wang, Lin Yu, Yan-Ping Li et al. "Concave-lens-like long-period fiber grating bidirectional high-sensitivity bending sensor." *Optics Letters* 42, no. 19 (2017): 3892-3895. https://doi.org/10.1364/OL.42.003892

[9] Zhang, Xinpu, Wei Peng, Li-Yang Shao, Wei Pan, and Lianshan Yan. "Strain and temperature discrimination by using temperature-independent FPI and FBG." *Sensors and Actuators A: Physical* 272 (2018): 134-138. https://doi.org/10.1016/j.sna.2018.01.060
[10] Sarkar, Sanjib, Mehdi Tarhani, Morad Khosravi Eghbal, and Mehdi Shadaram. "Discrimination between strain and temperature effects of a single fiber Bragg grating sensor using sidelobe power." *Journal of Applied Physics* 127, no. 11 (2020). https://doi.org/10.1063/1.5139041
[11] Portosi, Vincenza, Dario Laneve, Mario Christian Falconi, and Francesco Prudenzano. "Advances on photonic crystal fiber sensors and applications." *Sensors* 19, no. 8 (2019): 1892. https://doi.org/10.3390/s19081892
[12] Natesan, Ayyanar, Kuppusamy Peramandai Govindasamy, Thavasi Raja Gopal, Vigneswaran Dhasarathan, and Arafa Hussein Aly. "Tricore photonic crystal fibre based refractive index sensor for glucose detection." *IET Optoelectronics* 13, no. 3 (2019): 118-123. https://doi.org/10.1049/iet-opt.2018.5079
[13] Anelli, Francesco, Andrea Annunziato, Mike Godfrey, Antonella Maria Loconsole, Christopher Holmes, and Francesco Prudenzano. "Effects of Curvature on Flexible Bragg Grating in Off-Axis Core: Theory and Experiment." *Journal of Lightwave Technology* 41, no. 9 (2023): 2904-2910. https://doi.org/10.1109/JLT.2023.3238427
[14] Xu, Shishi, Hongliang Chen, and Wenlin Feng. "Fiber-optic curvature and temperature sensor based on the lateral-offset spliced SMF-FCF-SMF interference structure." *Optics & Laser Technology* 141 (2021): 107174. https://doi.org/10.1016/j.optlastec.2021.107174
[15] Wu, Yongfeng, Yundong Zhang, Jing Wu, and Ping Yuan. "Fiber-optic hybrid-structured Fabry–Perot interferometer based on large lateral offset splicing for simultaneous measurement of strain and temperature." *Journal of Lightwave Technology* 35, no. 19 (2017): 4311-4315. https://doi.org/10.1109/JLT.2017.2734062
[16] Wang, Qi, and Yu Liu. "Review of optical fiber bending/curvature sensor." *Measurement* 130 (2018): 161-176. https://doi.org/10.1016/j.measurement.2018.07.068
[17] Tan, XueMei, and Denis Rodrigue. "A review on porous polymeric membrane preparation. Part II: Production techniques with polyethylene, polydimethylsiloxane, polypropylene, polyimide, and polytetrafluoroethylene." *Polymers* 11, no. 8 (2019): 1310. https://doi.org/10.3390/polym11081310
[18] Gokaltun, Aslihan, Martin L. Yarmush, Ayse Asatekin, and O. Berk Usta. "Recent advances in nonbiofouling PDMS surface modification strategies applicable to microfluidic technology." *Technology* 5, no. 01 (2017): 1-12. https://doi.org/10.1142/S2339547817300013
[19] Akther, Fahima, Shazwani Binte Yakob, Nam-Trung Nguyen, and Hang T. Ta. "Surface modification techniques for endothelial cell seeding in PDMS microfluidic devices." *Biosensors* 10, no. 11 (2020): 182. https://doi.org/10.3390/bios10110182
[20] Shakeri, Amid, Shadman Khan, and Tohid F. Didar. "Conventional and emerging strategies for the fabrication and functionalization of PDMS-based microfluidic devices." *Lab on a Chip* 21, no. 16 (2021): 3053-3075. https://doi.org/10.1039/D1LC00288K
[21] Hwang, Juwon, Yeongjun Kim, Hyeondong Yang, and Je Hoon Oh. "Fabrication of hierarchically porous structured PDMS composites and their application as a flexible capacitive pressure sensor." *Composites Part B: Engineering* 211 (2021): 108607. https://doi.org/10.1016/j.compositesb.2021.108607
[22] Kim, Kang-Hyun, Soon Kyu Hong, Nam-Su Jang, Sung-Hun Ha, Hyung Woo Lee, and Jong-Man Kim. "Wearable resistive pressure sensor based on highly flexible carbon composite conductors with irregular surface morphology." *ACS Applied Materials & Interfaces* 9, no. 20 (2017): 17499-17507. https://doi.org/10.1021/acsami.7b06119
[23] Li, Dan, Jie Yao, Hao Sun, Bing Liu, Sjack van Agtmaal, and Chunhui Feng. "Recycling of phenol from aqueous solutions by pervaporation with ZSM-5/PDMS/PVDF hollow fiber composite membrane." *Applied Surface Science* 427 (2018): 288-297. https://doi.org/10.1016/j.apsusc.2017.08.202
[24] Jin, Meng-Yi, Yuan Liao, Choon-Hong Tan, and Rong Wang. "Development of high performance nanofibrous composite membranes by optimizing polydimethylsiloxane architectures for phenol transport." *Journal of Membrane Science* 549 (2018): 638-648. https://doi.org/10.1016/j.memsci.2017.10.051
[25] Cui, Xiaokun, Guiyu Zhu, Yufeng Pan, Qian Shao, Mengyao Dong, Yue Zhang, and Zhanhu Guo. "Polydimethylsiloxane-titania nanocomposite coating: Fabrication and corrosion resistance." *Polymer* 138 (2018): 203-210. https://doi.org/10.1016/j.polymer.2018.01.063
[26] Sondhi, Kartik, Seahee Hwangbo, Yong-Kyu Yoon, Toshikazu Nishida, and Z. Hugh Fan. "Airbrushing and surface modification for fabricating flexible electronics on polydimethylsiloxane." *Journal of Micromechanics and Microengineering* 28, no. 12 (2018): 125014. https://doi.org/10.1088/1361-6439/aae9d6
[27] Li, Yaomin, Lei Yuan, Hao Ming, Xin Li, Lin Tang, Jian Zhang, Ruichen Wang et al. "Enhanced hydrolytic resistance of fluorinated silicon-containing polyether urethanes." *Biomacromolecules* 21, no. 4 (2020): 1460-1470. https://doi.org/10.1021/acs.biomac.9b01768

[28] Mai, Huy, Rahim Mutlu, Charbel Tawk, Gursel Alici, and Vitor Sencadas. "Ultra-stretchable MWCNT–Ecoflex piezoresistive sensors for human motion detection applications." *Composites Science and Technology* 173 (2019): 118-124. https://doi.org/10.1016/j.compscitech.2019.02.001

[29] Pérez-Calixto, Daniel, Diego Zamarrón-Hernández, Aarón Cruz-Ramírez, Mathieu Hautefeuille, Juan Hérnandez-Cordero, Victor Velázquez, and Marcela Grether. "Fabrication of large all-PDMS micropatterned waveguides for lab on chip integration using a rapid prototyping technique." *Optical Materials Express* 7, no. 4 (2017): 1343-1350. https://doi.org/10.1364/OME.7.001343

[30] To, Celeste, Tess Hellebrekers, Jaewoong Jung, Sohee John Yoon, and Yong-Lae Park. "A soft optical waveguide coupled with fiber optics for dynamic pressure and strain sensing." *IEEE Robotics and Automation Letters* 3, no. 4 (2018): 3821-3827. https://doi.org/10.1109/LRA.2018.2856937

[31] Suslik, Lubos, Dusan Pudis, Matej Goraus, Rainer Nolte, Jaroslav Kovac, Jana Durisova, Peter Gaso, Pavol Hronec, and Peter Schaaf. "Photonic crystal and photonic quasicrystal patterned in PDMS surfaces and their effect on LED radiation properties." *Applied Surface Science* 395 (2017): 220-225. https://doi.org/10.1016/j.apsusc.2016.07.051

[32] Gao, Han, Haifeng Hu, Yong Zhao, Jin Li, Ming Lei, and Yong Zhang. "Highly-sensitive optical fiber temperature sensors based on PDMS/silica hybrid fiber structures." *Sensors and Actuators A: Physical* 284 (2018): 22-27. https://doi.org/10.1016/j.sna.2018.10.011

[33] Li, Changxu, Wenlong Yang, Min Wang, Xiaoyang Yu, Jianying Fan, Yanling Xiong, Yuqiang Yang, and Linjun Li. "A review of coating materials used to improve the performance of optical fiber sensors." *Sensors* 20, no. 15 (2020): 4215. https://doi.org/10.3390/s20154215

[34] Dahlberg, Tobias, Tim Stangner, Hanqing Zhang, Krister Wiklund, Petter Lundberg, Ludvig Edman, and Magnus Andersson. "3D printed water-soluble scaffolds for rapid production of PDMS micro-fluidic flow chambers." *Scientific reports* 8, no. 1 (2018): 1-10. https://doi.org/10.1038/s41598-018-21638-w

[35] He, Zhiwei, Yizhi Zhuo, Jianying He, and Zhiliang Zhang. "Design and preparation of sandwich-like polydimethylsiloxane (PDMS) sponges with super-low ice adhesion." *Soft Matter* 14, no. 23 (2018): 4846-4851. https://doi.org/10.1039/C8SM00820E